Bit Error Rate Analysis of OTDM System Based on Moment Generation Function

Jianfeng Zhang, Minyu Yao, Xingzhong Chen, Lei Xu, Minghua Chen, and Yizhi Gao

***Abstract*—The performance of optical time division multiplexing (OTDM) system is limited by a complex combination of noise. In this paper we present a theoretical framework for the optical receiver in OTDM system based on the moment generation function. The proposed receiver model is showed to be more accurate in predicting the bit error rate (BER) performance than the former ones. Its validity is also verified by the experimental results.**

***Index Terms*—Bit error rate (BER), demultiplexers, optical receivers, optical time division multiplexing (OTDM).**

I. Introduction

OPTICAL time division multiplexing (OTDM) is a very powerful technique for the ultrahigh-speed communication system. So far, some papers have been presented for the theoretical analysis of the bit error rate (BER) performance of the optical time division multiplexing (OTDM) system [1]–[4]. Reference [2] presents a detailed theoretical model for the receiver with an optical demultiplexer, in which the authors pointed out that the two factors, channel crosstalk, and relative timing jitter affected the system performance. Jepsen *et al.* [3] also showed experimentally that the interferometic noise would become a serious problem to degrade the BER performance when the pulses before multiplexing have a poor tail extinction ratio. So that the evaluation of OTDM system performance requires a composite consideration of the effects imposed by the channel crosstalk, timing jitter, and interferometic noise.

In the formerly proposed model [2], Gaussian approximation is made to evaluate the intensity noise generated by the timing jitter, some simplifications are also applied to include the channel crosstalk. Such assumption and simplification may bring about much inaccuracy in some cases. However, the exact analysis is complicated, since these noise sources mentioned above are nonadditive and nonstationary.

The need to accurately characterize system performance has led us to propose the theoretical model based on the moment generation function (MGF). This model deals with the actual probability distribution function of the noise related to the timing jitter, and evaluates the channel crosstalk in a more accurate way. The interferometic noise can also be easily included in this model.

Manuscript received February 11, 2000; revised June 21, 2000. This work was supported by Nature Science Foundation Committee of China (NSFC) (68738010) and High Technology Research and Development Program of China.

The authors are with the Department of Electronic Engineering, Tsinghua University, Beijing, China (e-mail: zhjf99@mails.tsinghua.edu.cn).

Publisher Item Identifier S 0733-8724(00)09818-2.

In Section II, we present this theoretical model in detail, the moment generation function for the decision variable is derived and saddle point approximation is introduced to calculate BER. In Section III, we evaluate the system performance based on this numerical model, and compare the results with other methods. In Section IV we describe an experiment to testify its validity. In Section V, summarizing conclusions are drawn.

II. Theoretical Model

At the receiving end of the OTDM transmission system, one of the multiplexed channels is first demultiplexed and then input into the optical receiver, just as Fig. 1 shows.

As for one channel, the optical field is given by

$$E_i = \sqrt{a_i} A(t-\tau_i) e^{i\phi(t-\tau_i)} \vec{r}_i \tag{1}$$

where a_i represents information bit, $a_i \in \{\rho, 1\}$. ρ is related to the extinction ratio of the optical modulator. $A(t)$ represents the field's envelope, τ_i represents the random timing jitter, r_i represents the polarization state.

If we assume the shape of the switching window is represented by $W(t)$, the electron intensity of the demultiplexed channel converted by the photodetector is given by

$$S_{\text{demux}} = \frac{1}{2}\frac{\eta}{hf}\left|\sum_{i=1}^{N}\sqrt{a_i}A(t-\tau_i)e^{i\phi_i(t-\tau_i)}\vec{r}_i\right|^2 \cdot W(t-\tau_w) \tag{2}$$

where

- τ_w timing jitter of switching window;
- η photodetector quantum efficiency;
- h Planck's constant;
- N number of the multiplexed channels.

Equation (2) can be expanded further as

$$S_{\text{demux}} = \frac{1}{2}\frac{\eta}{hf}\left[\sum_{i=1}^{N} a_i A^2(t-\tau_i)W(t-\tau_w) + \sum_{i=1}^{N}\sum_{j=i+1}^{N}\sqrt{a_i a_j}A(t-\tau_i)A(t-\tau_j) \cdot \cos(\Delta\phi_{ij})W(t-\tau_w)\vec{r}_i \bullet \vec{r}_j\right]. \tag{3}$$

From (3), we can notice that three factors affect the performance of the received signals, as shown in Fig. 2.

1) Channel crosstalk: if the switching window $W(t)$ have an imperfect extinction ratio, other channels may leak into the receiver, as the first term in (3) shows.

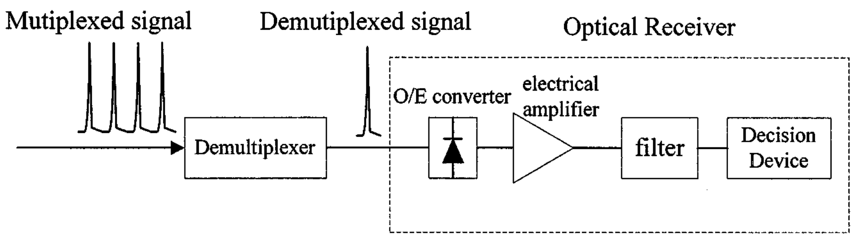

Fig. 1. OTDM receiver model.

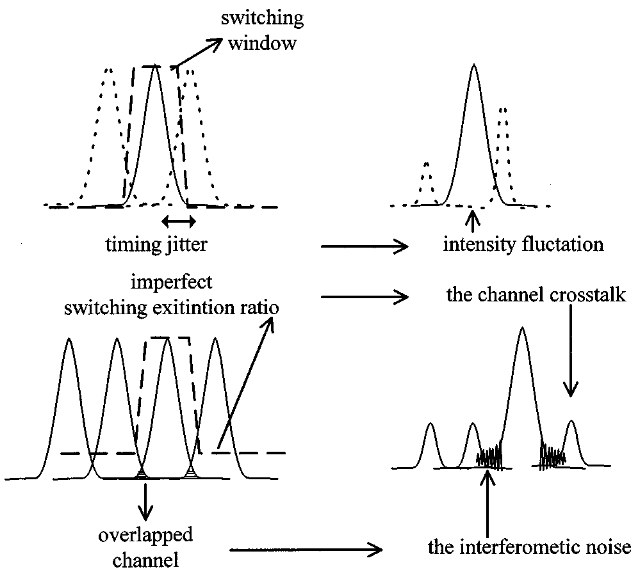

Fig. 2. The major factors degrading the received signal in OTDM system.

2) Timing jitter: $\vec{\tau} = (\tau_1, \tau_2, \ldots, \tau_i, \ldots, \tau_N, \tau_w)$ results in intensity fluctuations through the demultiplexer.
3) Interferometic noise: if the relative phase difference $\Delta\phi_{ij}$ fluctuates, the output will be added by the intensity noise.

After O/E conversion, the demultiplexed signal is electrically amplified and filtered, then sampled and input into the decision device. The converted electrical signal is modeled as a marked and filtered Poisson process $Y(t)$ [9], thus its conditioned moment generation function is given by

$$M_Y(s, \vec{a}, \vec{\tau}, \overrightarrow{\Delta\phi}) = \exp\left\{\int_{-\infty}^{\infty} S_{\text{demux}} \cdot [M_g(h(t-t')s) - 1]\, dt'\right\} \quad (4)$$

where $\vec{a} = (a_1, a_2, \ldots, a_i, \ldots, a_N)$ is a vector in which each a_i represents the information bit of each multiplexed channel, $\vec{\tau} = (\tau_1, \tau_2, \ldots, \tau_i, \ldots, \tau_N, \tau_w)$ represents the series of random timing jitter variables. While $\overrightarrow{\Delta\phi}$ represents phase noise vector, $h(t)$ is the impulse response of the postamplifier filter. $M_g(s)$ is the moment generation function associated with the photodetector. As for PIN and APD detectors, they have different MGFs. For simplicity, we assume the PIN photodetector, thus $M_g(s)$ is given by

$$M_g(s) = \exp(s). \quad (5)$$

The electrical filter is assumed with a rectangular impulse shape

$$h(t) = \begin{cases} 1 & 0 < t < T \\ 0 & \text{elsewhere} \end{cases} \quad (6)$$

where T is the symbol period at the base rate.

With the above assumptions, (4) can be simplified

$$M_Y(s, \vec{a}, \vec{\tau}, \overrightarrow{\Delta\phi}) = \exp\left\{\int_0^T S_{\text{demux}}(e^s - 1)\, dt'\right\} \quad (7)$$

In the presence of channel crosstalk, timing jitter noise and interferometic noise, the filtered Poisson process Y's moment generation function is given by averaging all possible information, jitter, and phase noise vectors

$$M_Y(s) = \frac{1}{2^{N-1}} \sum E_\tau(E_{\Delta\phi}(M_Y(s, \vec{a}, \vec{\tau}))) \quad (8)$$

where $E(\bullet)$ is the expectation operator representing statistical averaging.

The converted signal is also corrupted by the Gaussian thermal noise $n(t)$ originating in the electrical amplifier. The sampled Gaussian process at the input to the decision circuit is modeled by a random variable N with MGF [9]

$$M_N(s) = \exp\left(\frac{\sigma_{th}^2 s}{2}\right) \quad (9)$$

where σ_{th} represents the variance of the thermal noise. The total random variable Z at the input to the decision circuit is the result of addition of statistically independent random variable Y and N,

$$M_Z(s) = M_Y(s) \bullet M_N(s). \quad (10)$$

Equations (4)–(10) provide a complete description of the signal and noise processes at the decision times in terms of symbol-conditioned MGF. The significant stochastic impairments encountered in OTDM system are accommodated, these equations thus provide a sound foundation on which to base accurate performance evaluation methods. Several bounds and approximation methods for the evaluation of average error probability have been proposed, such as modified Chernoff bound (MCB), Gauss quadrature rule (GQR), and saddlepoint approximation (SAP) [6], [7]. In this paper, we apply SAP to evaluate the noise performance, which can result in satisfactory accuracy. We outline here briefly the general form of this method.

In terms of the MGF of the random variable Z, the probability density function of Z can be got by the Laplace transformation, thus the BER can be given by

$$P_{e0}(z) = \frac{1}{2\pi}\int_{c_0-i\infty}^{c_0+i\infty} M_{Z_0}(s)e^{-Ds}\,ds \qquad C_0 > 0 \tag{11a}$$

$$P_{e1}(z) = \frac{1}{2\pi}\int_{c_1-i\infty}^{c_1+i\infty} M_{Z_0}(s)e^{-Ds}\,ds \qquad C_1 < 0 \tag{11b}$$

where D is the decision threshold. One takes $c_0 = s_0$ and $c_1 = s_1$, where s_0 and s_1 are saddlepoints, the integrands of (11a) and (11b) can be approximated as

$$P_{e_{0,1}} = \frac{\exp[\psi_{0,1}(s_{0,1})]}{\sqrt{2\pi\psi''_{0,1}(s_{0,1})}} \tag{12}$$

with primes indicating differentiation, where

$$\psi_{0,1} = \ln(M_{Z_{0,1}}(s_{0,1})) - \ln(s_{0,1}) - sD. \tag{13}$$

The optimized decision threshold D and saddlepoints s_0, s_1 can be got numerically by solving a set of equations [6]

$$\frac{d\psi_{0,1}(s)}{ds} = 0 \tag{14}$$

$$\frac{dP_e}{dD} = 0. \tag{15}$$

We employed the Newton–Raphson algorithm to solve the equations (14) and (15).

III. Performance Analysis

In the presence of channel crosstalk, timing jitter, and interferometic noise, the system performance is evaluated based on this model, and the comparison with the theoretical model adopted by reference [2] is also given. In the calculations, we assume the signal pulse width is equal to be 1/5 of the time slot width and the power penalty is calculated at $\text{BER} = 10^{-9}$.

A. Timing Jitter

The relative timing jitter between the signal and the switching window leads to fluctuations in transmittance of the signal and thus degrades the system performance. Large timing jitter can result in the error floor in BER performance [1].

To include the intensity noise generated by the timing jitter into the receiver model easily, the noise is usually assumed to be of Gaussian distribution [2]. However, this assumption is questionable. The model based on the MGF takes the actual PDF of noise into consideration, and the calculation shows different results in evaluating the effect of timing jitter.

In the calculation, the switching window is assumed to be square and equal to the width of the time slot. Results have been calculated for two jitter distributions, which are Gaussian distribution and triangular distribution. As Fig. 3 shows, we observe a very significant difference between our results and those predicted by the Gaussian approximation.

This is especially marked for the Gaussian timing jitter, where the Gaussian approximation considerably underestimates the influence of timing jitter. This difference stems from the fact that the actual PDF of the signal fluctuations has more weight in its tail than a Gaussian PDF. The triangular timing jitter is less damaging due to its finite distribution, however, the calculated difference between two methods is also obvious. For the practical system, the timing jitter of optical signal is usually of Gaussian distribution. Experiments have shown that the tolerable variance of timing jitter should be no more than 1/12 of switching window width to achieve $\text{BER} < 10^{-9}$ [5], which is in agreement with this model.

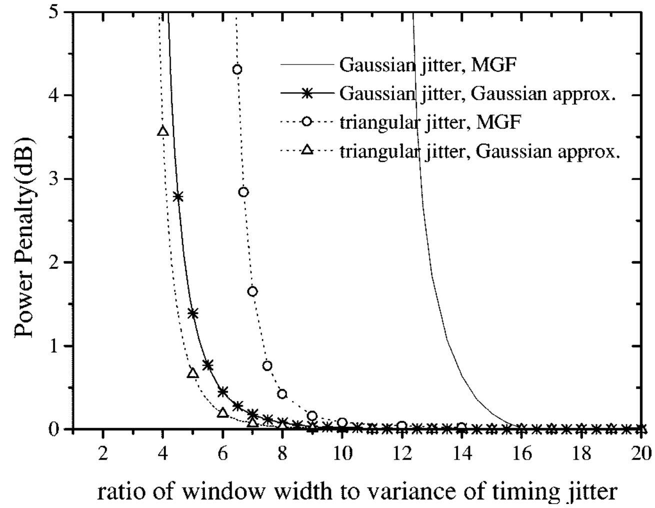

Fig. 3. Predicted system performance in the presence of timing jitter by using MGF method and Gaussian approximation. The switching window is assumed to be square and equal to the width of the time slot.

B. Channel Crosstalk

The channel crosstalk reduces the extinction ratio of the received signal, thus it degrades the system performance. Notice that the amount of the channel crosstalk is also related to the corresponding data pattern $(a_1, a_2, \ldots, a_i, \ldots, a_N)$, thus the output signal is also added by the pattern-related intensity noise.

However, the channel crosstalk is usually evaluated with the assumption that the channels contributing to crosstalk are all in mark “1” mode [1], [2]. For the extinction ratio of the received signal, it is the worst-case data pattern. Moreover, the pattern noise is also neglected in this way. In this paper, by averaging the sequence-conditioned MGFs on all possible data patterns, the crosstalk can be evaluated in a more accurate way.

Fig. 4 shows the relation between the power penalty and the extinction ratio of switching window predicted by using this two models. As we see, with window’s extinction ratio decreasing, or the multiplexing number increasing, the power penalty is increased as predicted by both models, and the worst-case data pattern usually predicts a worse performance. As for the small multiplexing numbers ($N = 4$), the difference between the calculated results by this two model is small, When the multiplexing number is increased ($N = 10$), the maximum difference is approximately as 1 dB. However, if the extinction ratio is poor ($<$ 10 dB), the predicted performance will be similar. We give the explanation in this way. As the worst-case pattern assumption only counts the case of one data pattern, obviously, the calculated difference will be greater if the number of crosstalk channels is increased. However, as the switching window’s extinction ratio becomes poor, the pattern dependent

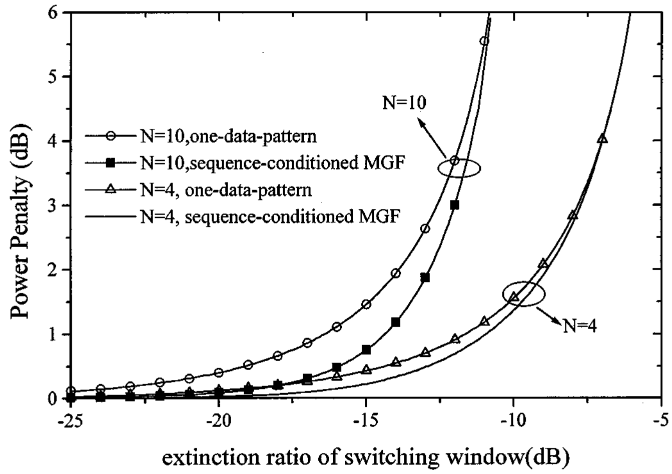

Fig. 4. Predicted system performance in the presence of channel crosstalk by using one-data-pattern assumption and sequence-conditioned MGFs. In the calculation, the switching window width is assumed to have an explicit relation to the extinction ratio, just as that of a NOLM demultiplexer does.

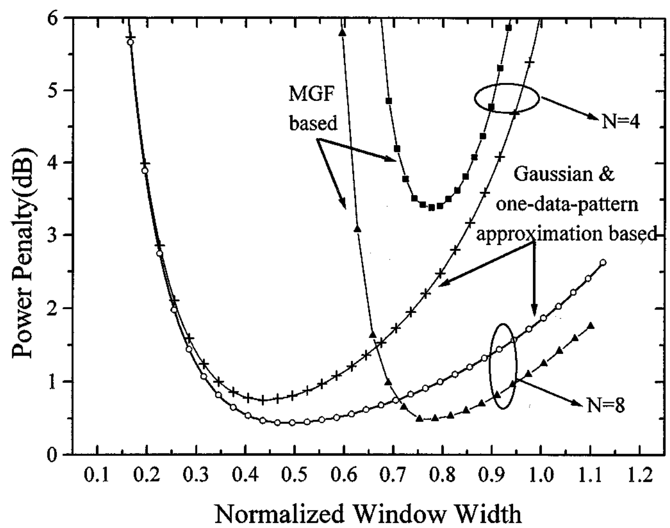

Fig. 5. System performance related to the switching window predicted by two models. The relative timing jitter is assumed to be 1/20 of the time slot width. The switching window is normalized by the time slot width.

noise neglected by one-data-pattern assumption may dominate, so the compromise is achieved and the difference becomes less.

From the Fig. 4, we can conclude that for the system with a large number of multiplexed channels and for a certain range of switching extinction ratio (-20 dB ~ -10 dB), a more accurate method that not only considering the worst data pattern should be applied.

Using this model, We can also investigate the system performance when both the channel crosstalk and timing jitter noise dominates. Compared with former models based on the Gaussian approximation and one-data-pattern assumption [1] [2], this model is more suitable for the optimization of system performance.

In the following, we show the optimization of the switching window width of a NOLM demultiplexer for the system by using this model. The relative timing jitter is assumed to be 1/20 of the time slot width. As Fig. 5 shows, the predicted performances related to the switching window width by the two models differ greatly. The optimized window width predicted by the model based on Gaussian and one-data-pattern approximation is much smaller than the model proposed by this paper, which is due to that it underestimates the effect of timing jitter greatly. If the window width is comparatively large, for large multiplexing numbers ($N = 8$), the predicted performance by the conventional model is worse, it is due to the fact that the channel crosstalk dominates under this condition and this model overestimates the channel crosstalk. Note that for the same normalized window width, the system with larger mulitplexing rate ($N = 8$) has less timing jitter and higher switching extinction ratio, thus it has a better performance.

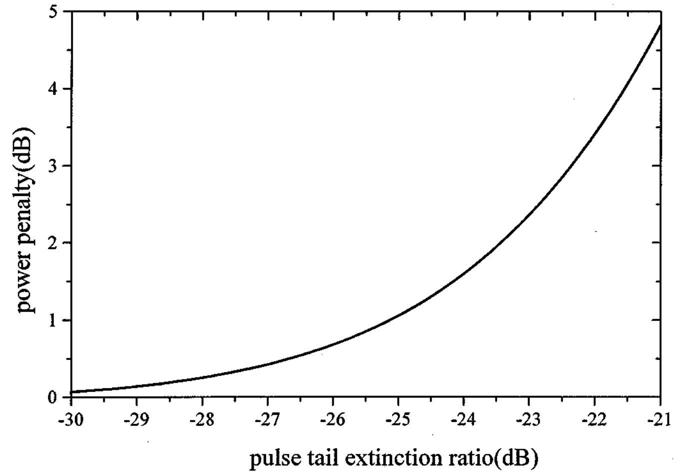

Fig. 6. The effect of interferometic noise on system performance. The switching window is assumed to be square and equal to the width of the time slot.

From the above analysis, we can conclude that the Gaussian approximation and one-data-pattern assumption adopted by the formerly proposed model may result in much inaccuracy in some cases and the model based on MGF can be applied in these cases.

C. Interferometic Noise

In the actual system, it is often the truth that the closest neighboring channels contribute most to the interferometic noise due to the pulse pedestal or long tail. Due to the fact that the number of interferometic sources is small, the noise distribution deviates far from the Gaussian distribution [8]. However, based on MGF, we can easily evaluate the interferometic noise in the presence of other specific noises for OTDM system.

With the assumption that only the neighboring channels contributing to the interferometic noise and the interacting pulses are of the same polarization, (3) can be simplified as

$$S_{\text{demux}} = \frac{1}{2}\frac{\eta}{hf}\left[\sum_{i=1}^{N} a_i A^2(t-\tau_i)W(t-\tau_w) + 2\sqrt{\varepsilon_1 a_1 a_N}A^2(t-\tau_1)W(t-\tau_w)\cos(\phi_1) + 2\sqrt{\varepsilon_2 a_1 a_2}A^2(t-\tau_1)W(t-\tau_w)\cos(\phi_2)\right] \tag{16}$$

where ε_1 and ε_2 represent the falling and rising tail extinction ratio, respectively.

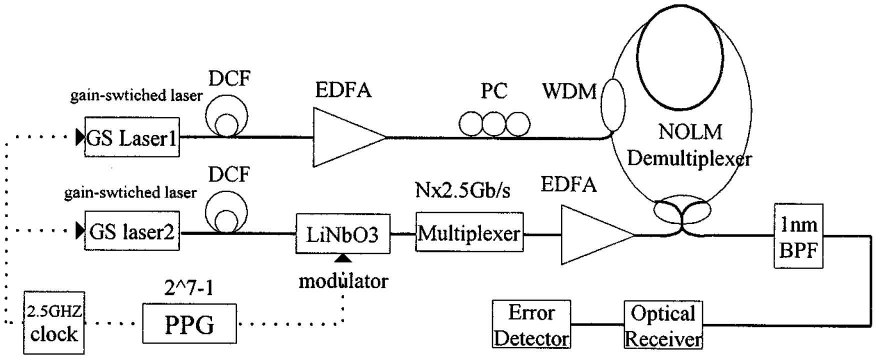

Fig. 7. Experimental setup.

The distribution of phase noise is assumed to have a Gaussian shape

$$f(\Delta\phi) = \frac{1}{\sqrt{2\pi\Delta\nu\Delta\tau}} \exp\left(-\frac{\Delta\phi^2}{2(\Delta\nu\Delta\tau)}\right) \qquad (17)$$

where $\Delta\nu$ is variance of the signal phase noise, and $\Delta\tau$ is the delay difference between the multiplexed channels.

In the calculation, ε_1 is assumed to be equal to ε_2, and $\Delta\nu\Delta\tau \gg 1$, thus the distribution is uniform between $[-\pi, \pi]$. Fig. 6 shows the effect of the interferometic noise on the system performance. We can see that when the tail extinction ratio is above -25 dB, the resulted power penalty will increase drastically. For the transmission system in which the phase of channels are incoherent and pulses have a poor extinction ratio, the effect of interferometic noise can not be neglected.

IV. Experimental Results and Discussion

The experimental setup is shown in Fig. 7. Signal pulses and control pulses were generated by two gain-switched lasers sinusoidally modulated at 2.5 GHz, and linearly compressed by the dispersion compensation fiber (DCF). The width of the compressed pulses is 11 ps. The signal pulses were externally modulated by a $LiNbO_3$ intensity modulator with a 20–dB extinction ratio and then time-division multiplexed eight times in a fiber interleaver. The control pulses were amplified to an average power of about 15 mw and input into the NOLM demultiplexer. The demultiplexed signal was detected by a P-I-N photodetector and finally the BER was measured by the error detector.

In the experiment, the timing jitter variance of the optical pulses was measured by the digital sampling oscilloscope (Tek11801C). The relative timing jitter was measured to be 1.2 ps. Various types of NOLM demultiplexers with walk-off time 4 ps, 18 ps, and 53 ps were used to investigate the system in different conditions when channel crosstalk or timing jitter noise may dominate. The corresponding fiber loop length was 2 km, 3 km, and 9 km.

Measured and theoretical bit error rate curves for different values of width of switching window are presented in Fig. 8. For walk-off time 4 ps and 18 ps, the corresponding switching window is relatively narrow, which could not suppress the timing jitter noise, so error floors at BER $= 10^{-7}$ and 10^{-11} were observed. For large walk-off time 53 ps, the error floor was suppressed below 10^{-12}, however, the increased channel crosstalk due to the wider switching window resulted in a large power penalty of 2 dB. As shown in Fig. 8, the numerical results calculated by the model based on MGF are in good agreement with the experimental ones. The results calculated by the methods used in reference [2] are also shown in the figure. It can be observed that the analysis using a Gaussian distribution may yield great discrepancies if the relatively great timing jitter noise exists in system. For NOLM with 53 ps switching window, although the timing jitter resulted noise can be neglected, the predicted performance are not in good agreement with the actual one due to the one-data-pattern assumption it adopts to evaluate the channel crosstalk.

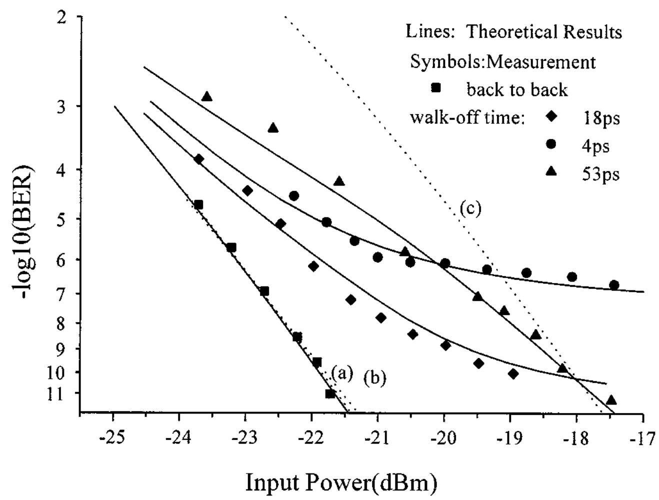

Fig. 8. System BER performance for different switching windows. The solid lines are theoretical curves calculated by MGF, the dotted lines (a) (b) (c) are calculated by the methods in [2], which is corresponding to different walk–off time 18 ps, 12 ps, and 53 ps.

To investigate the system performance in the presence of interferometic noise, the signal pulses generated by the GS-DFB laser were multiplexed as two channels by a fiber interleaver, one path of which is composed by an adjustable delay line. At the receiving end, one channel was demultiplexed by the NOLM demultiplexer (the walk-off time is 18 ps), the other channel functioned as the interferometic noise source. Obviously, as the interval between the two channels reduced, the interferometic noise had a greater detrimental effect on the system.

The insets in Fig. 9 shows the eye-diagrams of the multiplexed channels (25 ps interval) and the demultiplexed channel,

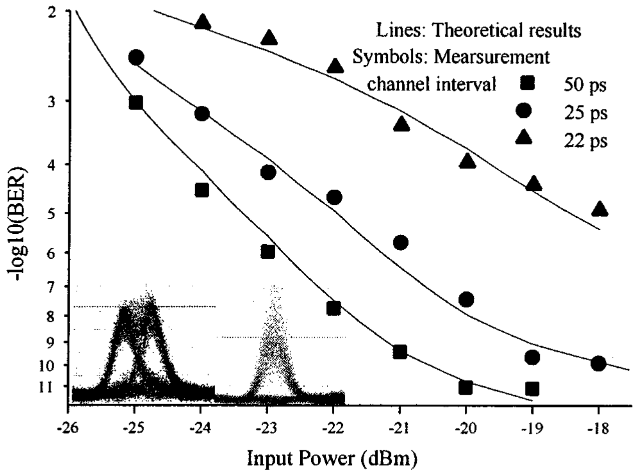

Fig. 9. System BER performance in the presence of interferometic noise. Symbols denote the measurement BER data. The solid lines are the theoretical curves. The insets show the diagrams of the overlapped channel and the demultiplexed channel with interferometic noise. The walk-off time of the NOLM demultiplexer is 18 ps.

we can see the presence of the interferometic noise as the pulses overlapped. In the experiment the interval between the channels varied between 50–20 ps, polarization states of two channels were matched to simulate the worst case situation. Both theoretical and experimental results show that the interferometic noise degrades the system performance greatly, and they are in good agreement.

V. Conclusion

The performance analysis for OTDM system in the presence of timing jitter, channel crosstalk, and interferometic noise has been studied by using the model based on MGF. The expression for the MGF of the decision variable is derived and saddle point approximation is introduced to calculate the average BER. The supporting experiments simulate the system in different conditions and show good agreement with the theoretical results.

Acknowledgment

The authors would like to thank their colleagues for technical support and discussions.

References

[1] M. Jinno, "Effects of crosstalk and timing jitter on all-optical time-division demultiplexing using a nonlinear fiber sagnac interferometer switch," *IEEE J. Quantum Electron.*, vol. 30, pp. 2842–2853, Dec. 1994.

[2] K. Uchiyama, T. Morioka, S. Kawanishi, H. Takara, and M. Saruwatari, "Signal-to-noise ratio analysis of 100 gb/s demultiplexing using nonlinear optical loop mirror," *J. Lightwave Technol.*, vol. 15, pp. 194–201, Feb. 1997.

[3] K. S. Jepsen, H. N. Poulsen, A. T. Clausen, A. Buxens, and K. E. Stubkjaer, "Investigation of cascadability of add-drop multiplexers in otdm systems," in *Proc. ECOC'98*, 1998, pp. 619–620.

[4] D. Zhou, K. Kang, I. Glesk, and P. R. Prucnal, "An analysis of signal-to-noise ratio and design parameters of a terahertz optical asymmetric demultiplexer," *J. Lightwave Technol.*, vol. 17, Feb. 1998.

[5] K. Uchiyama, H. Takam, T. Morioka, S. Kawanishi, and M. Saruwatari, "Effects of control-signal pulse walk-off on BER performance of nonlinear optical loop mirror demultiplexer," *Electron. Lett.*, vol. 29, pp. 1313–1314, 1993.

[6] G. Einarsson, *Principles of Lightwave Communications*. New York: Wiley, 1996.

[7] A. A. Al-Orainy and J. J. O'Reilly, "Error probability and approximations for the influence of crosstalk on wavelength division multiplexed systems," *Inst. Elect. Eng. Proc. J. Optoelectron.*, vol. 137, no. 6, pp. 379–384, 1990.

[8] I. T. Monory and E. Tangdiongga, "Performance evaluation of optical cross-connects by saddlepoint approximation," *J. Lightwave Technol.*, vol. 16, pp. 317–323, Mar. 1998.

[9] J. J. O'Reilly and R. F. Rocha, "Improved error probability evaluation methods for direct detection optical communication systems," *IEEE Trans. Inform. Theory*, vol. IT-33, pp. 839–848, June 1987.

Jianfeng Zhang, photograph and biography not available at the time of publication.

Minyu Yao, photograph and biography not available at the time of publication.

Xingzhong Chen, photograph and biography not available at the time of publication.

Lei Xu, photograph and biography not available at the time of publication.

Minghua Chen, photograph and biography not available at the time of publication.

Yizhi Gao, photograph and biography not available at the time of publication.